

Formation of quartic solitons and a localized continuum in silicon-based slot waveguides

Samudra Roy and Fabio Biancalana

Max Planck Institute for the Science of Light, Günther-Scharowsky-Strasse 1, Bau 26, 91058 Erlangen, Germany

(Received 26 September 2012; published 6 February 2013)

We explore the possibility of exciting the so-called quartic solitons in specially designed slot waveguides based on silicon and silica or silicon nanocrystals. This requires the excitation of the structure with quasi-transverse-magnetic polarized pulses—for which the Raman effect is absent—and at a specific infrared wavelength for which only the second- and fourth-order group velocity coefficients are nonvanishing. Pulses launched in these conditions will generate a spectrally localized continuum coming from the spectral interference of many quartic solitons.

DOI: [10.1103/PhysRevA.87.025801](https://doi.org/10.1103/PhysRevA.87.025801)

PACS number(s): 42.65.Tg, 05.45.Yv, 42.65.Ky

Starting from 1993, Höök, Karlsson, Buryak, and Akhmediev [1–4] demonstrated theoretically the existence of a family of solitary wave solutions of the equation

$$i\partial_z A - \frac{1}{2}\beta_2\partial_t^2 A + \frac{1}{24}\beta_4\partial_t^4 A + \gamma|A|^2 A = 0, \quad (1)$$

where $A(z, t)$ is the electric field envelope, $\beta_{2,4}$ are, respectively, the second- and fourth-order group velocity dispersion (GVD) coefficients of the waveguide calculated at a reference frequency ω_0 (taken to be the central frequency of the input pulse), and γ is the nonlinear coefficient of the fundamental fiber mode. Equation (1) is valid when ω_0 is located at a local maximum (or minimum) of the GVD, where β_3 vanished identically. The properties of such peculiar solitary waves—which are dubbed *quartic solitons* (Qs)—have been since then studied in detail. It was found that Qs exist only for $\beta_{2,4} < 0$, can have or not have oscillating decaying tails, and can form symmetric (in-phase) and antisymmetric (out-of-phase) bound states, and that only the single-peak solitons can be stable [2–5].

In principle, it would be possible to design specific solid-core photonic crystal fibers (PCFs) [6] with a quartic profile of the GVD as required by Eq. (1) by using, for instance, the dispersion-flattened fibers reported in Ref. [7], or the nanobore fibers reported in Ref. [8]. However, the perturbation induced by the Raman effect would completely destroy the Qs. Indeed, from the very beginning of the propagation, their central frequency would continuously translate due to the intrapulse Raman self-frequency shift [9], thus moving all solitons away from the point at which $\beta_3 = 0$, which immediately breaks the validity of Eq. (1). This is mainly the reason why the above theoretical works have been considered only as a mathematical curiosity, only marginally discussed in textbooks [10,11], and largely forgotten during the past two decades.

However, the recent advent of silicon photonics [12–15] has opened many interesting possibilities in nonlinear optics, mainly due to its potential applications in the spectral region extending from the near- to the mid-infrared. The high refractive index of silicon, combined with the silicon-on-insulator (SOI) technology, allows a tight confinement of the optical modes and a consequent increase of the nonlinear coefficient of the waveguide, enabling efficient nonlinear optical interactions at low power levels and in relatively short length.

In this Brief Report we propose a feasible way to observe and use the generation of Qs in specially designed

silicon-based waveguides. The two structures that we propose—both of which are built on a silica substrate—have been inspired by Refs. [16,17] and are depicted in Figs. 1(a) and 1(b). In Fig. 1(a) we show the structural parameters of our silicon-silica (Si-SiO₂) waveguide, where the GVD for quasi-transverse-electric (TE) and quasi-transverse-magnetic (TM) modes and the mode profile for the quasi-TM mode are also shown. In Fig. 1(b) we show the same information as in Fig. 1(a), but for our silicon-silicon nanocrystals (Si-SiNc) waveguide. The gray-shaded circles, centered at the wavelengths λ_0 at which $\beta_3(\lambda_0) \simeq 0$ (which will be referred to as the *quartic point*), are the regions around which the GVD can be approximated by including only β_2 and β_4 in the dispersion. Note that in those regions, the dispersion is anomalous ($\beta_2 < 0$), the GVD curvature is negative ($\beta_4 < 0$), and β_3 is as small as 1.9×10^{-5} ps³/m [for the structure of Fig. 1(a)]. As described above, these are exactly the necessary conditions for the possible existence of localized Qs, and the parameters of the structure must be carefully designed in order to achieve the correct sign and curvature of the GVD at the desired wavelength.

Apart from the shape of the GVD, one must consider the impact of the two-photon absorption (TPA) generated by the free carriers around λ_0 . As demonstrated in numerous experimental works (see, e.g., Refs. [18–21]), the impact of TPA is greatly reduced if $\lambda_0 > 2.2$ μm , away from the two-photon band edge, where the three-photon absorption is also insignificant [19–21].

The final crucial property for the present work is that for an SOI waveguide fabricated along the $[\bar{1}10]$ direction on the $[110] \times [001]$ surface, stimulated Raman scattering (SRS) cannot occur when an input pulse excites the quasi-TM mode of the waveguide [15,22]. Thus, for pulses launched close to $\lambda_0 = 2\pi c/\omega_0$, the nonlinearity is dominated by the Kerr effect and is not affected by the carrier dynamics, and the dimensionless propagation equation can be thus written as

$$i\partial_\xi \psi + \sum_{m \geq 2} i^m \delta_m \partial_\tau^m \psi + (1 + is\partial_\tau)|\psi|^2 \psi = 0, \quad (2)$$

where we have performed the typical scalings $A \equiv \sqrt{P_0}\psi$, $t \equiv t_0\tau$, and $z \equiv z_0\xi$, where $z_0 = t_0^2/|\beta_2|$, $\delta_m \equiv \beta_m/(m!|\beta_2|t_0^{m-2})$, β_m is the m^{th} order dispersion coefficient, $P_0 \equiv (\gamma z_0)^{-1}$, and $s \equiv (\omega_0 t_0)^{-1}$, with t_0 being the input pulse duration [10]. In

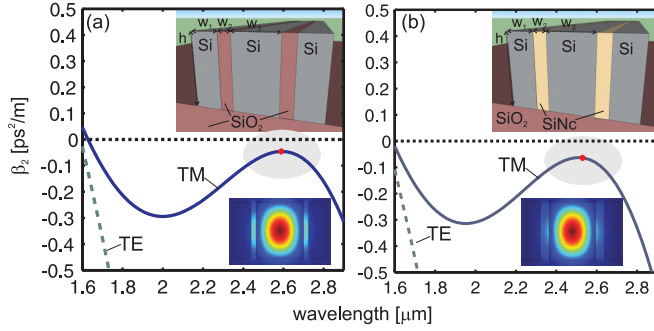


FIG. 1. (Color online) The silicon-based structures (both on a SiO_2 substrate) studied in this Brief Report. (a) GVD of quasi-TE (dashed line) and -TM (solid line) modes of the Si- SiO_2 slot waveguide. Inset below: TM-mode profile at $\lambda_0 = 2592$ nm. Inset above: geometry and materials of the structure. Parameters are $h = 700$ nm, $w_1 = 220$ nm, $w_2 = 60$ nm, $w_3 = 600$ nm. (b) GVD of quasi-TE (dashed line) and -TM (solid line) modes of the Si-SiNc slot waveguide. Inset below: TM-mode profile at $\lambda_0 = 2511$ nm. Inset above: geometry and materials of the structure. Parameters are $h = 700$ nm, $w_1 = 190$ nm, $w_2 = 80$ nm, $w_3 = 570$ nm. In both figures, the red dot indicates the wavelength λ_0 at which $\beta_3 = 0$, and the gray area is the region where the quartic approximation of the GVD, and therefore the use of Eq. (2), is valid.

Eq. (2) coefficients δ_2 and δ_4 are dominant and both negative, while $|\delta_3| \ll 1$ in proximity of the quartic point. γ is the nonlinear coefficient of the structure calculated with a mode solver. For subwavelength waveguides with large refractive index contrast between core and cladding, the nonlinear parameter is defined as $\gamma = k(\epsilon_0/\mu_0) \int n^2(x, y) n_2(x, y) [2|\mathbf{e}_v|^4 + |\mathbf{e}_v^2|^2] dA / (3 \int (\mathbf{e}_v \times \mathbf{h}_v^*) \cdot \hat{z} dA)^2$ [23]. We have calculated the individual components of the integral using COMSOL and integrate it over the silicon core region where the optical mode is confined tightly.

In Eq. (2), it was very important to take into account the *shock operator* that multiplies the Kerr nonlinear term, which comes directly from the Maxwell equations when using a perturbative reduction to the envelope [24]. The shock operator introduces a nonlinear change in the group velocity, due to which different parts of the pulse travel at different velocities, leading eventually to optical shocks [10]. Such an operator considerably influences the dynamics in those situations where the Raman effect is absent, as in the present case. This constitutes the main difference between Eq. (1) and Eq. (2), the latter having now a direct physical interpretation in the systems studied here. It is therefore crucial to check that the shock term does not destroy the QSs around the quartic point where third-order dispersion (3OD) is negligible. To verify this for the structure of Fig. 1(a), we launched an input pulse $\psi_{\text{in}} = N \text{sech}(\tau)$ at wavelength $\lambda_0 = 2.6 \mu\text{m}$ in the simulation of Eq. (2), and propagated it for several dispersion lengths, see Fig. 2, in the absence [Fig. 2(a)] and in the presence [Fig. 2(b)] of the shock operator, for the parameters indicated in the caption. At this point it should be noted that for Fig. 2(b) the full model of Eq. (2) is used where 3OD is also included in the simulation. However, the effect of the latter is found to be negligible since the optical pulse is launched in the vicinity of the quartic point. It is clear by comparing these two figures that the shock term has the effect modifying the velocity of each

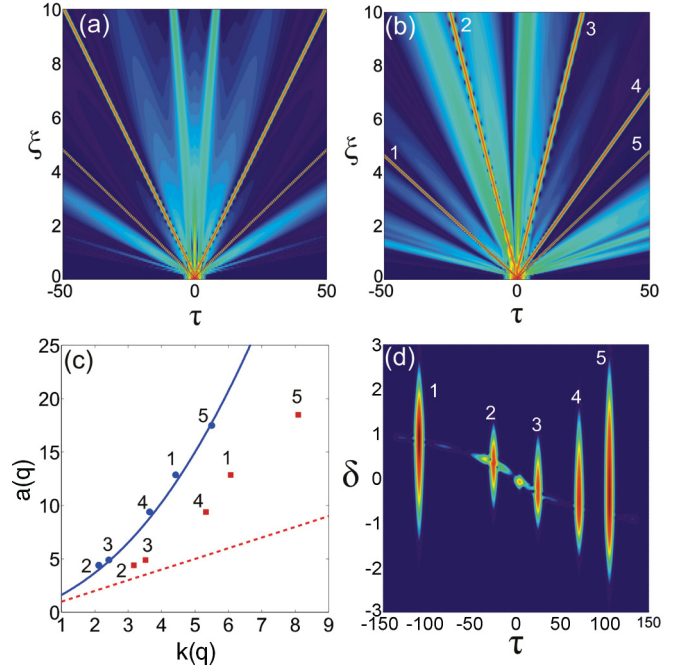


FIG. 2. (Color online) (a) Propagation of an input pulse $\psi_{\text{in}} = N \text{sech}(\tau)$, with $N = 10$ and $\delta_4 = -0.01$, no shock term ($s = 0$) and no 3OD ($\delta_3 = 0$). Due to the nonintegrability of Eq. (2), which induces the presence of a solitonic friction, the pulse splits into several fundamental quartic solitons, approximated by Eqs. (3) and (4). (b) Same as in (a), but in the presence of a shock term ($s = 0.03$) and 3OD ($\delta_3 = 0.0017$). The shock term induces an asymmetric splitting of the solitons, which all decrease their velocity with respect to the case of (a). (c) Position of the parameters (a, k) of each soliton formed in (b) after a propagation distance $\xi = 10$ (dots), on the predicted curve calculated by using Eqs. (3) and (4), indicated with a solid line. The dashed line indicates the relation between $a(q)$ and $k(q)$ that would exist for conventional Schrödinger solitons, for which $a(q) = k(q)$. The squares indicate the extracted parameters $a(q)$ and $k(q)$ obtained by fitting with a function $f = a(q) \text{sech}[k(q)\tau]$. It is therefore evident that all the localized structures formed [which are numbered from 1 to 5 in (b)–(d)] are quartic solitons and not simple Schrödinger solitons. (d) XFROG spectrogram of (b) at $\xi = 10$.

individual QS, without affecting its shape or stability during the propagation, and actually allowing the generation of more solitons than what occurs in the case of $s = 0$. To verify this fact, we compare the approximate analytical nonoscillating solutions of Eq. (2), for $s = 0$ and $\delta_3 = 0$, obtained via variational methods, with the actual solitons produced in the simulations (with $s \neq 0$ and $\delta_3 \neq 0$). Such solutions are given by Ref. [4] $\psi(\xi, \tau) = f(\tau) e^{iq\xi}$, where q is the nonlinear wave number, $f = a(q) \text{sech}^2[k(q)\tau]$, with $a(q)$ and $k(q)$ being the two functions

$$a(q) \equiv \left[\frac{7}{3} k^2(q) + \frac{80}{3} |\delta_4| k^4(q) \right]^{1/2}, \quad (3)$$

$$k(q) \equiv \left[\frac{\sqrt{9 + 400|\delta_4|q} - 3}{80|\delta_4|} \right]^{1/2}. \quad (4)$$

The solid line in Fig. 2(c) shows the relation between $k(q)$ and $a(q)$ given by Eqs. (3) and (4), while the dots indicate the parameters of the solitons extracted with a fit from the

simulation (numbered from 1 to 5) given in Fig. 2(b) in the (a, k) space. One can see that the dots are very well predicted by the solid line, indicating the formation of true QSs in the simulations. To exclude that these are just conventional Schrödinger solitons, in Fig. 2(c) we also plot a dashed line indicating the relation $f = a(q)\text{sech}[k(q)\tau]$ for $a(q) = k(q)$, which is a straight line. When we extract (by means of a hyperbolic secant fit) the values of $a(q)$ and $k(q)$ of each soliton from the simulation of Fig. 2(b), we obtain the squares shown in Fig. 2(c). These are not placed in correspondence with the dashed line and are not even placed on a straight line as it should be for Schrödinger solitons, therefore demonstrating that what we see are true QSs. In Fig. 2(d) we show the cross-correlation frequency resolved optical gating (XFROG) spectrogram of the propagation shown in Fig. 2(b), for a propagation distance $\xi = 10$. XFROG is a standard technique used to represent ultrashort pulses in frequency and time domain and is defined as the convolution $S(\tau, \omega, \xi) = |\int_{-\infty}^{\infty} \psi(\xi, \tau') \psi_{\text{ref}}(\tau - \tau') \exp(i\omega\tau') d\tau'|^2$, where ψ_{ref} is the reference window function, generally taken as the input pulse [10]. From the XFROG the separation of the different QSs in both space and frequency is evident. As we describe below, each soliton acquires a small frequency shift from the quartic point. The correct dispersion experienced by each soliton is naturally taken automatically into account in the full Eq. (2), since the dispersion operator changes its value according to the individual frequency of each pulse.

Finally, in Fig. 3 we show the propagation of a $t_0 = 40$ fs pulse in the structure of Fig. 1(a), for $\lambda_0 = 2.6 \mu\text{m}$, with other parameters reported in the caption. The pulse propagation simulation has been obtained by solving the full Eq. (2) using a common split-step Fourier algorithm with a fourth-order Runge-Kutta for the nonlinear part [10]. Energetic femtosecond lasers at the infrared frequencies considered in this work are commonly made of chromium-doped crystals [25]. The formation of a continuum extending from approximately 2 to 3 μm is the consequence of the strong spectral interference between many QSs forming near the quartic point of the GVD, which are close in the frequency domain due to the absence of the Raman effect (and thus of any deceleration that can act on the solitons, followed by a continuous self-frequency shift [9]) for the chosen quasi-TM input polarization. Each of the solitons in Fig. 2(d) undergoes a small frequency shift from the quartic point, which can be either positive or negative, due to the initial splitting of pulses. Therefore, each soliton experiences a different group velocity, as can be seen by recalculating the Taylor expansion in the dispersion operator

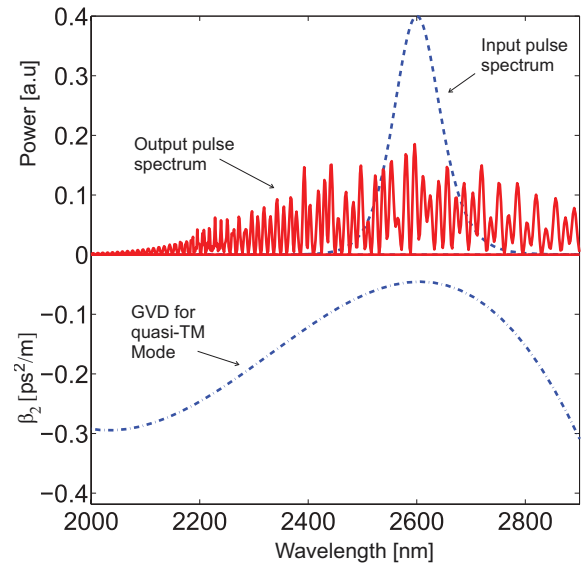


FIG. 3. (Color online) Formation of a QS-induced continuum. The bottom part shows the GVD (dashed-dotted line) of the quasi-TM mode vs wavelength for the structure shown in Fig. 1(a). The top part shows the input pulse spectrum (dotted line) and the output spectrum (solid red line) after a propagation of $\xi = 10$. Input pulse duration is $t_0 = 40$ fs, input wavelength is $\lambda_0 = 2.6 \mu\text{m}$, at which $\beta_2 \simeq -0.05 \text{ ps}^2/\text{m}$, $\beta_3 \simeq 1.9 \times 10^{-5} \text{ ps}^3/\text{m}$, and $\beta_4 \simeq -2.5 \times 10^{-5} \text{ ps}^4/\text{m}$. The nonlinear coefficient for the structure of Fig. 1(a) is calculated by using the vector model of Ref. [23], and is $\gamma \simeq 42 \text{ m}^{-1} \text{ W}^{-1}$. The corresponding fundamental power is $P_0 = 0.74 \text{ W}$. Input pulse shape is $N\text{sech}(t/t_0)$, with soliton order $N = 5$.

in Eq. (2). However, it is interesting (and surprising) to note that the quartic solitons are robust and do not tend to become Schrödinger solitons, as demonstrated clearly in Fig. 2(c). Therefore, Fig. 2(d) cannot be interpreted as a conventional pulse splitting of Schrödinger solitons as in Ref. [26].

In conclusion, we have demonstrated analytically and numerically the possibility of the observation of localized quartic solitons in specially designed silicon-based slot waveguides. The absence of the Raman effect for TM-polarized pulses, together with specific structures that allow a quartic GVD curve to be realized far from the two-photon absorption region of silicon, permits the generation of many nonradiative QSs and the formation of a spectrally localized continuum around the quartic point of the GVD.

This research was funded by the Max Planck Society for the Advancement of Science (MPG).

[1] A. Höök and M. Karlsson, *Opt. Lett.* **18**, 1388 (1993).
 [2] M. Karlsson and A. Höök, *Opt. Comm.* **104**, 303 (1994).
 [3] N. N. Akhmediev, A. V. Buryak, and M. Karlsson, *Opt. Comm.* **110**, 540 (1994).
 [4] A. V. Buryak and N. N. Akhmediev, *Phys. Rev. E* **51**, 3572 (1995).
 [5] M. Piché, J. F. Cornier, and X. Zhu, *Opt. Lett.* **21**, 845 (1996).
 [6] P. St. J. Russell, *Science* **299**, 358 (2003).

[7] W. H. Reeves *et al.*, *Nature* **424**, 511 (2003).
 [8] T. G. Euser *et al.*, *J. Opt. Soc. Am. B* **28**, 193 (2011).
 [9] F. M. Mitschke and L. F. Mollenauer, *Opt. Lett.* **11**, 659 (1986); J. P. Gordon, *ibid.* **11**, 662 (1986).
 [10] G. P. Agrawal, *Nonlinear Fiber Optics*, 4th ed. (Academic, San Diego, 2007).
 [11] G. P. Agrawal, *Optical Solitons: From Fibers to Photonic Crystals* (Academic, San Diego, 2003).

- [12] *Silicon Photonics*, edited by L. Pavesi and D. J. Lockwood (Springer, New York, 2004).
- [13] B. Jalali, *J. Lightwave Technol.* **24**, 4600 (2006).
- [14] M. Lipson, *Nanotechnol.* **15**, S622 (2004).
- [15] Q. Lin, O. J. Painter, and G. P. Agrawal, *Opt. Express* **15**, 16604 (2007).
- [16] L. Zhang *et al.*, *Opt. Express* **18**, 20529 (2010).
- [17] L. Zhang *et al.*, *Opt. Express* **20**, 1685 (2012).
- [18] A. D. Bristow, N. Rotenberg, and H. M. van Driel, *Appl. Phys. Lett.* **90**, 191104 (2007).
- [19] X. Liu *et al.*, *Opt. Express* **19**, 7778 (2011).
- [20] B. Jalali *et al.*, *IEEE J. Sel. Top. Quant. Electron.* **12**, 1618 (2006).
- [21] V. Raghunathan *et al.*, *Opt. Express* **15**, 14355 (2007).
- [22] Q. Lin *et al.*, *Opt. Express* **14**, 4786 (2006).
- [23] S. Afshar V. and T. M. Monro, *Opt. Express* **17**, 2298 (2009).
- [24] T. Brabec and F. Krausz, *Phys. Rev. Lett.* **78**, 3282 (1997).
- [25] F. Druon, F. Balembos, and P. Georges, *C. R. Phys.* **8**, 153 (2007).
- [26] A. V. Husakou and J. Herrmann, *Phys. Rev. Lett.* **87**, 203901 (2001).